Distinguishing Enolic and Carbonyl Components in the Mechanism of Carboxylic Acid Ketonization on Monoclinic Zirconia

ARTICLE *in* ACS CATALYSIS · JULY 2012

Impact Factor: 9.31 · DOI: 10.1021/cs3002989

2 AUTHORS:

Alexey V. Ignatchenko
University of North Dakota
14 PUBLICATIONS **166** CITATIONS
SEE PROFILE

Kozliak Evguenii
University of North Dakota
7 PUBLICATIONS **50** CITATIONS
SEE PROFILE

ACS Catalysis

Research Article

pubs.acs.org/acscatalysis

Distinguishing Enolic and Carbonyl Components in the Mechanism of Carboxylic Acid Ketonization on Monoclinic Zirconia

Alexey V. Ignatchenko*[,†,‡] and Evguenii I. Kozliak[‡]

[†]Energy & Environmental Research Center, Stop 9018, and [‡]Department of Chemistry, Stop 9024, University of North Dakota, Grand Forks, North Dakota 58202, United States

Supporting Information

ABSTRACT: This study contributes toward understanding the mechanism of catalytic formation of mixed ketones in an attempt to improve their selectivity vs symmetrical ketones. A pulsed microreactor placed inside a gas chromatograph−mass spectrometer instrument was used to identify the source of carbonyl group and quantify its distribution among products of zirconia-catalyzed cross-ketonization reaction of a mixture of carboxylic acids, with the carbonyl group of one of the acids selectively labeled by ^{13}C. A concept of enolic and carbonyl components in the ketonization mechanism was introduced to distinguish the sources of alkyl and acyl groups, respectively. The least branched acid was found to be the predominant source of CO_2, the essential byproduct of ketonization. Thus the least branched acid is the preferred source of the alkyl group of the cross-ketone product, while the most branched acid provides the acyl group. Increased branching at the α carbon next to the carbonyl group decreased the reactivity of both the enolic and the carbonyl components. Following a pseudo first order kinetic analysis, the relative reaction rates for a common enolic component with a pair of different carbonyl components were measured by the method of competing reactions to obtain mechanistic insights. The distinction between two possible paths in the cross-ketonization mechanism was characterized quantitatively by assessing the difference in activation energies; the results obtained were explained by the steric effect of substituents. On the basis of detailed kinetic analysis, the rate-limiting step most likely occurs after the enolic component activation.

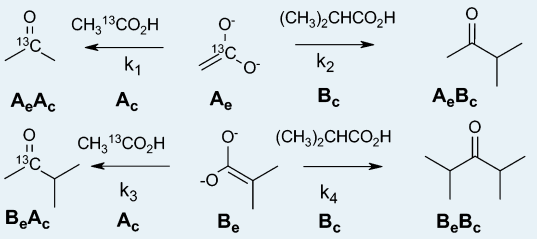

KEYWORDS: *ketonic decarboxylation, decarboxylative ketonization, ketonization mechanism, surface ketene, carboxylic acid enolization, kinetic study*

1. INTRODUCTION

Vapor-phase ketonization of carboxylic acids on metal oxide catalysts has a great potential as an economically competitive and environmentally friendly industrial process.[1−4] Ketones, such as acetone, methyl ethyl ketone, methyl isobutyl ketone, and cyclohexanone, are used as solvents and intermediates in electronic, agricultural, and pharmaceutical industries.[5] The noncatalytic version of ketonic decarboxylation is a classic organic chemistry reaction, one of the first known since organic chemistry separated into a specific science.[6] Details on the preparation of the simplest ketone, acetone, by calcium acetate pyrolysis were published for the first time in 1858 by Friedel,[7] although this reaction had been mentioned in earlier publications and practiced for several centuries prior to that.[6] Almost concurrently, Fittig communicated that other metal carboxylates can be used and that a variety of other ketones can be prepared by this general method.[8] In this stoichiometric version of this reaction, a metal oxide is a byproduct of the carboxylate ketonization; however, later it was found that merely a catalytic amount of the metal oxide at high temperatures can convert carboxylic acids into ketones. During research efforts stretched over 150 years, oxides of almost all Group 1−4 metals have been tested as catalysts (literature examples are reviewed in refs 9−12).

An important observation in the pyrolysis of metal carboxylates is that the yield of decarboxylative ketonization increases when an excess of the carboxylic acid relative to the metal oxide is used.[3] The same rule applies to the catalytic ketonization on the surface of nonsoluble metal oxides.[13] Thus during pulse chemisorption studies on samarium oxide, the first portions of acetic acid are intensively adsorbed on the surface.[14] No ketonization products are formed until a certain degree of the surface saturation is reached. The rate of acetone formation, however, does not depend on the concentration of acetic acid in the gas phase, for which a zero kinetic order is observed. Instead, it is proportional to the concentration of surface species.[15−18] The second-order dependence of ketonization rate was observed on a ceria−zirconia catalyst only at a small partial pressure of hexanoic acid, less than 0.1 atm, while partial pressures above 0.1 atm yielded the zero-order kinetics.[19] To explain these observations, the adsorption of acids followed by their specific transformation on the surface, that is, activation, must happen prior to its reaction with the second acid molecule.[20] The second molecule could be either adsorbed

Received: May 11, 2012
Revised: June 14, 2012

   dx.doi.org/10.1021/cs3002989 | ACS Catal. 2012, 2, 1555−1562

nearby on surface (Langmuir–Hinshelwood mechanism) or supplied from the gas phase (Rideal–Eley mechanism). It has been suggested that the ketonization of acetic acid follows the Langmuir–Hinshelwood mechanism with ferric oxide catalysts[21] as well as with mixed oxides of iron, zinc, and chromium.[22]

Speculative mechanisms of carboxylic acid ketonization on various metal oxides were extensively discussed during the 20th century and reviewed in the literature.[3,11,20] Without going into details, we would like to emphasize here a common aspect that is shared between all of the proposed mechanisms. The pivotal point is that the product ketone is constructed of two nonequivalent fragments, acyl and alkyl groups. During the course of reaction, these two structurally different components are combined into one ketone product and have to be distinguished. Only one of these components supplies the carbonyl group whereas the other one provides the alkyl group. On the basis of the analogy with the classic aldol condensation, these two fragments may be called the carbonyl and the enolic components, respectively. Inclination toward mechanisms assuming enolization of surface carboxylates as the initial activation step, is common in the most recent publications.[10,23,24] It is postulated that the enolized form of the surface carboxylate attacks nucleophilically the carbonyl group of the second carboxylic acid.[10] Obviously, the enolized form of a carboxylate is a stronger nucleophile and is expected to be more reactive toward electrophiles than the original carboxylate. It has been demonstrated that an alkaline treatment of metal oxide catalysts improves their ketonization activity,[1,25,26] thus indicating that the base catalyzed enolization of surface carboxylates could be an essential part of the ketonization mechanism. In a number of studies, enolization of surface carboxylates was evidenced during the exchange of their alpha protons for deuterium.[10,11,27,28] Exchange of alpha hydrogen atoms under basic conditions mechanistically can take place only through the enolization of carboxylates followed by protonation of the enolized fragment as depicted in Scheme 1.

Scheme 1. H/D Exchange of Alpha Hydrogen Atoms in Surface Carboxylates through Their Enolization

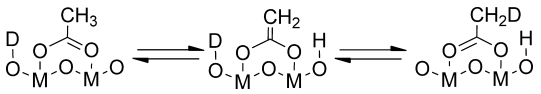

The feasibility of a facile enolization of carboxylic acids adsorbed on monoclinic zirconia catalyst surfaces was demonstrated in a recent computational study by one of us.[29] The calculated activation energies for the enolization of carboxylates on zirconia, 25–32 kcal/mol, turned out to be comparable to the experimental value of the Arrhenius activation energy for the catalytic ketonization of carboxylic acids on various metal oxides, for example 33.5 kcal/mol for acetic acid on iron oxide,[30] 31.5 kcal/mol for hexanoic acid on ceria–zirconia catalyst,[19] and 28.0 kcal/mol for acetic acid on zirconium oxide in the present study. Resemblance of these values raises a question whether the enolization could be the rate-limiting step in the ketonization mechanism, which controls the activation energy of the entire process.

Valuable mechanistic information can be obtained by monitoring the formation of nonsymmetrical ketones from a pair of different acids (i.e., cross-ketonization). Economical factors, for example, significantly higher prices of such nonsymmetrical ketone products,[26] provide an additional motivation for such a study. Several studies with isotopically labeled acids have been devoted to the identification of the carbonyl group source in the resulting nonsymmetrical ketone structure.[31−33] Prior research indicates that the preferred source of the ketone's carbonyl group is the most substituted carboxylic acid, while the alkyl group is preferentially provided by the least substituted acid.[10,24,31] Unfortunately, this effect has not been quantified as would be essential for selecting the most plausible mechanism.

Without detailed and targeted kinetic studies, any proposed mechanism remains speculative. To provide definitive mechanistic insights, the reaction kinetics leading to the same product by two different paths have to be measured and compared. We postulate that this is possible using the proposed setup. Kinetic studies aimed at a separate testing of the enolic and carbonyl component reactivity could shed more light on the steric and electronic factors governing the ketonization mechanism. It might also help to identify the rate-limiting step and suggest approaches to increase the reactivity and improve the selectivity of the mixed ketone formation.

In the current study, we developed a method allowing for a mechanistic discrimination between two possible paths of the cross-ketonization product formation and to measure relative rates in a competing reaction of the same enolic component with two different acids as the carbonyl components. We shall demonstrate here how the reaction rates of the enolic component can be measured without knowing its concentration on the catalyst surface and without the need to identify its exact structure. The obtained kinetic data provided a basis for the analysis and discrimination of various potential mechanisms.

2. EXPERIMENTAL SECTION

Materials. Acetic, propionic, isobutyric, and trimethylacetic acids, as well as two different isotopically labeled acetic acids, $^{13}CH_3{}^{13}CO_2H$, 99 atom % ^{13}C and $CH_3{}^{13}CO_2H$, 99 atom % ^{13}C, were purchased from Aldrich. Monoclinic zirconium oxide was purchased from Alfa Aesar. The Brunauer–Emmett–Teller (BET) surface area of the monoclinic zirconia catalyst, 48 m^2/g before and 45 m^2/g after a KOH treatment, was determined by the Micromeritics materials analysis laboratory.

Catalyst Preparation. Zirconium oxide catalyst pellets, 10 g, were soaked in 10 mL of 10% solution of KOH in water for 24 h at 60 °C under vacuum. The KOH solution was then drained; the catalyst was washed three times with 20 mL of deionized water, dried at 130 °C for 4 h, and calcined at 450 °C for 2 h at a 1 °C/min heating rate. Pellets were crushed and sieved. A fraction with a particle size of 0.25–0.71 mm was collected and used for carboxylic acid pulse chemisorption and ketonization studies.

Methods. The in situ, that is, placed inside a gas chromatograph (GC), pulse microreactor was used as previously described.[34,35] A small amount of the catalyst, 40 ± 1 mg, was placed inside the injection sleeve of the gas chromatograph–mass spectrometer (GC–MS) instrument described below in this section, exactly at the same location for all experiments, with the bottom of the catalyst bed being 10 mm above the bottom of the injection sleeve. The catalyst bed was held in place by deactivated glass wool, both on the top and bottom. A typical catalyst bed size was 10–13 mm in length and 2.0 mm in diameter. The preheating section length was 7–10 mm. The reactor with the catalyst was kept at a

dx.doi.org/10.1021/cs3002989 | ACS Catal. 2012, 2, 1555–1562

certain GC inlet temperature of each experiment, 200°−400 °C, for at least 15 min before the first injection to ensure the complete desorption of water and gases. An Agilent 7683 series automatic injector was used to feed acids into the reactor in pulses. The vapors' residence time was controlled by changing the total flow and the split ratio to ensure a constant column flow.

An HP 7890 gas chromatograph equipped with J&W Scientific 30 m DB-1 capillary column, 0.25 mm in diameter, thermal conductivity detector, and Agilent mass selective detector connected in parallel was used for the carboxylic acid pulse chemisorption and for the carboxylic acids switching studies in the cross ketonization reaction.

The employed GC analysis method used a constant column flow, 0.9 mL/min, split mode of injection with a split ratio of 100:1, helium carrier gas with a total flow of 92 mL/min through the catalyst bed, an oven temperature of 50 °C holding for 1 min and then rising 15 °C/min. Each GC run time was 7.67 min. The time between the pulses was 11−12 min. The amounts of all ketone products were calculated using the integration of the corresponding peaks, with external calibration.

Pulse Chemisorption. A carboxylic acid, 0.1 μL, was injected 20−40 times at temperatures 200°−400 °C until reaching the sample saturation evidenced by a plateau on the graph of the total amount of all GC-registered products. The amount of the adsorbed acid was calculated by integrating the peaks of all products exiting the reactor and subtracting it from the total amount of the acid injected. Essential corrections were made to account for the stoichiometric coefficients in the ketonization reaction.

Carboxylic Acid Switching Protocol. A 0.5 μL portion of the first acid, R^1CO_2H, was injected 5 times to saturate the catalyst surface at 250°−400 °C. Then, 0.1 μL of the second acid, R^2CO_2H, was injected 30−40 times until all products containing alkyl group R^1 were displaced as indicated by reaching a plateau on the graph for the products containing alkyl group R^2. The ratio of isotopes in the mixed ketone product was monitored by the mass selective detector specified above.

Continuous Flow Reactor. Steady-state experiments were conducted in the same microreactor by using continuous feed. For this purpose, helium carrier gas was saturated with reactant vapors by passing it at room temperature through a glass wool wetted by a selected carboxylic acid. The flow rate of the saturated helium through the catalyst bed was 92 mL/min. The duration of each run at various temperatures was 10 min. Concentration of all products was constantly monitored by the MS detector using the same GC analysis method as above, except for a constant oven temperature, 90 °C. The final concentration measurement at the end of the 10 min run was used to determine the reaction rate.

3. RESULTS AND DISCUSSION

3.1. Catalyst Surface Coverage by Carboxylates. During the catalytic ketonization of carboxylic acids, the catalyst surface is covered by a certain amount of carboxylates being at temperature-dependent equilibrium with the gas-phase acid. The surface coverage by carboxylic acids was determined by a modified pulse chemisorption technique. For this purpose, pulses of a given carboxylic acid were passed through the catalyst bed at a certain temperature until reaching surface saturation and equilibrium. The adsorbed acid was gradually replaced by adding a different acid, as described in the Experimental Section under the carboxylic acid switching protocol. Acetic acid was selected as the second acid in all such experiments. The amount of the carboxylic acid was measured by the GC−MS analysis as described above. Switching from the isotopically labeled $^{13}CH_3{}^{13}CO_2H$ to the regular acetic acid, CH_3CO_2H, was used to determine the adsorption capacity for acetic acid.

Adsorption capacities for carboxylic acids with a varied degree of branching, RCO_2H, on the zirconia catalyst are shown in Figure 1. These data were then compared with the

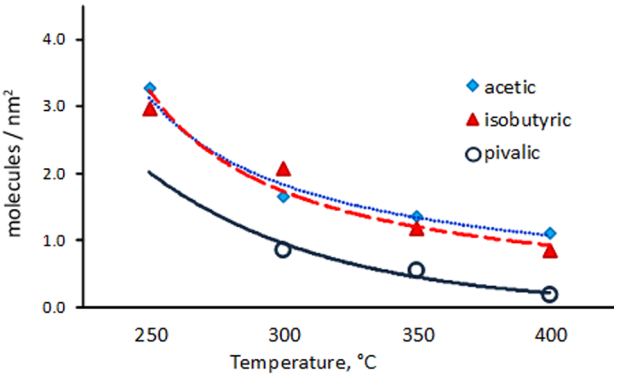

Figure 1. Surface concentration of carboxylic acids replaced by AcOH on KOH treated ZrO_2 catalyst depending on temperature, molecules per nm^2.

previously calculated theoretical concentration of Zr atoms on the most important monoclinic zirconia surfaces, $(\bar{1}11)$ and (111), which are 8.8 nm^{-2} and 7.9 nm^{-2}, respectively.[29] On this basis, the surface coverage calculated from the experimental data ranged from 13% to 42% for acetic acid, 10% to 38% for isobutyric acid, and only 2% to 11% for pivalic acid within a temperature range of 400°−250 °C. The coverage decreased with the temperature increase, as expected. A higher degree of acid branching at the α-carbon next to the carboxylic group resulted in a smaller surface coverage. This effect was particularly pronounced for pivalic acid. The difference between acetic and isobutyric acid coverage was not significant. An approximately equal surface coverage by isobutyrate and acetate indicates that the difference in the concentration of the corresponded enolized structures would be due only to the difference in their enolization equilibrium constants and the molar ratio of the two acids employed. This observation is discussed in the analysis of possible reasons for the different reactivity of acetic and isobutyric acids in Section 3.5.

It should be noted that the water coverage for monoclinic zirconia determined by the same technique[35] was of the same order of magnitude as for acetic and isobutyric acids. However, the relative adsorption of water, as compared to that of acids, was higher at 400 °C and lower at 250 °C. This difference can be explained by greater adsorption energies of carboxylic acids,[29,35] which are counterbalanced by their higher reactivity at high temperatures relative to the water adsorption energy and reactivity.

3.2. Apparent Activation Energy for Symmetrical Ketones Formation. The same pulse mode was used for the bulk of kinetic/mechanistic studies. In preliminary experiments, it was found that acetic acid is much more reactive than isobutyric acid. It is a general trend that a more

dx.doi.org/10.1021/cs3002989 | ACS Catal. 2012, 2, 1555−1562

branched acid is less reactive in making ketones.[12] Noticeable ketonization of acetic acid into acetone started at 180 °C with a KOH-treated zirconia catalyst in the pulse reactor, while the lowest temperature for detectable isobutyric acid ketonization to 2,4-dimethylpentan-3-one in the same reactor was 240 °C. Ketones were the only type of products observed with the KOH treated zirconia catalyst. High selectivity toward ketones with this catalyst has been previously described in literature.[25,26] The temperature dependence of the reaction rates for each individual acid, that is, the Arrhenius $\ln(k)$ vs $1/T$ plot obtained within a 225−300 °C range in the pulse reactor is shown in Figure 2. The slope of each graph yielded the apparent activation energy for symmetrical ketones, 14.0 ± 0.3 kcal/mol for acetone and 30.9 ± 0.5 kcal/mol for 2,4-dimethylpentan-3-one, respectively.

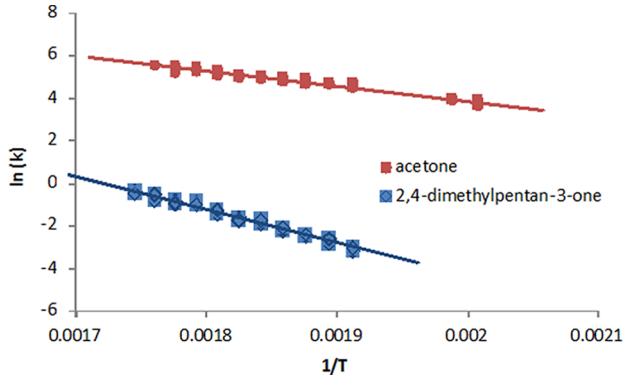

Figure 2. Temperature dependence of the rate constant in $\ln(k)$ vs $1/T$ coordinates for acetone and 2,4-dimethylpentan-3-one formation measured in the 225−300 °C range in a pulse microreactor.

For comparison, we measured the temperature dependence of the reaction rates in a continuous-flow system in exactly the same microreactor with the same catalyst. Activation energies in the continuous flow, that is, under steady-state conditions, appeared to be higher: 28.0 ± 1.6 kcal/mol for acetone and 46.0 ± 2.5 kcal/mol for 2,4-dimethylpentan-3-one formation. A similar difference between the activation energies obtained in pulse and continuous-flow reactors was observed on samarium oxide.[14] Most likely, the observed difference is due to a much longer residence time in the pulse mode, extended by the time between pulses. An additional factor could be a low concentration of proton sources between pulses. Under such nonsteady-state conditions, a greater portion of adsorbed carboxylates could be activated through their enolization, because fewer proton sources are available to convert the enolized species back to carboxylates. By contrast, a competing protonation reaction is always enabled in the continuous-flow reactor, helping to establish equilibrium between the carboxylates and their enolized forms. Therefore, in the pulse mode, the concentration of enolized carboxylates may be higher than in the continuous-flow mode, which would affect the measured value of the apparent activation energy. Despite this difference, the use of a pulse reactor for kinetic studies is justified because activation energies for the formation of all ketone products change proportionally upon the transition from a nonstationary to a stationary system.[14]

3.3. Paths "*a*" and "*b*" in the Cross-Ketonization Mechanism. A mixture of acetic acid labeled by ^{13}C on its carbonyl group and nonlabeled isobutyric acid was converted to a mixture of symmetrical and nonsymmetrical ketones in the pulse microreactor with the zirconia catalyst. Products were analyzed by GC−MS as described in the Experimental Section. The cross ketonization product, methyl isopropyl ketone, contained two isotopically different molecules with m/z of 86 and 87 (Scheme 2). Obviously, isotopologues $\mathbf{B_eA_c}$ and $\mathbf{A_eB_c}$

Scheme 2. Product Distribution and Pathways for the Cross-Ketonization Reaction of Isobutyric Acid, B, with Acetic Acid, A, Having ^{13}C Labeled Carbonyl Group[a]

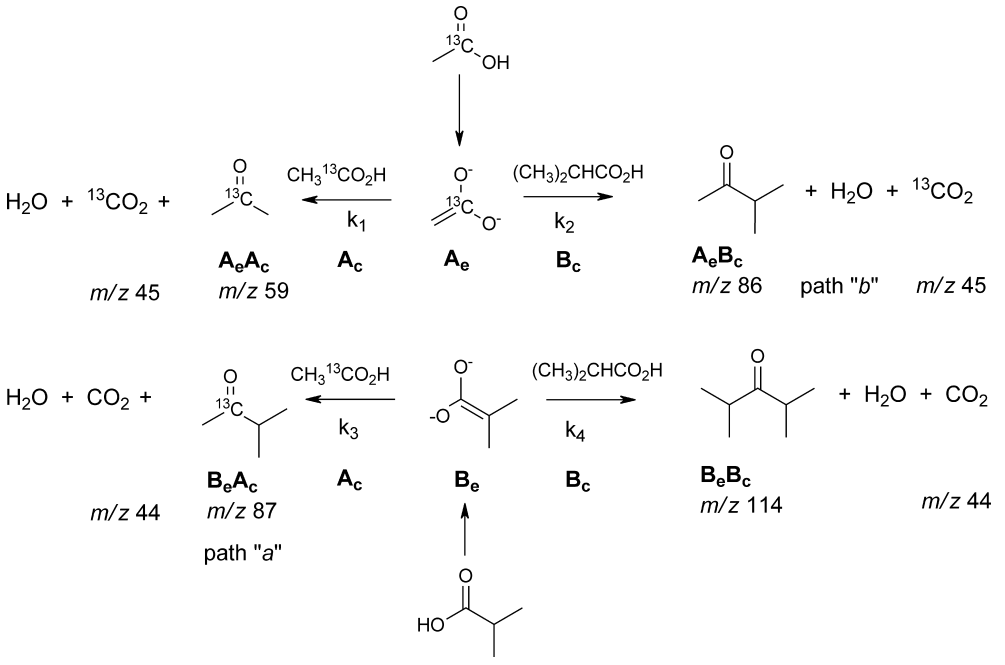

[a]Subscripts *e* and *c* designate enolic and carbonyl components, respectively.

dx.doi.org/10.1021/cs3002989 | ACS Catal. 2012, 2, 1555−1562

represent the same product, methyl isopropyl ketone, although formed by two different Paths, "*a*" and "*b*". Acetic acid, as the carbonyl component, yielded a GC−MS peak of *m*/*z* 87 following mechanistic Path "*a*". By contrast, acetic acid as the enolic component was the source of a different GC−MS peak of *m*/*z* 86 formed according to Path "*b*", as shown in Scheme 2.

In a direct way, two mechanistic paths were compared at various conditions by calculating their ratio from the concentration of mixed ketones with and without an isotope label on the carbonyl group (*m*/*z* 86 and *m*/*z* 87 in the case of isobutyric and acetic acid reaction, Scheme 2). In addition to isobutyric acid, cross-ketonization of the labeled acetic acid was studied with propionic and pivalic acids. The fraction of Path "*b*" in cross-ketonization of acetic acid with three different acids, calculated as $\mathbf{A_eB_c}/(\mathbf{A_eB_c} + \mathbf{B_eA_c})$, is shown in Figure 3 as a function of temperature. The preference for Path "*b*" increases with increased branching at the α carbon of the carboxylic acid and declines with temperature.

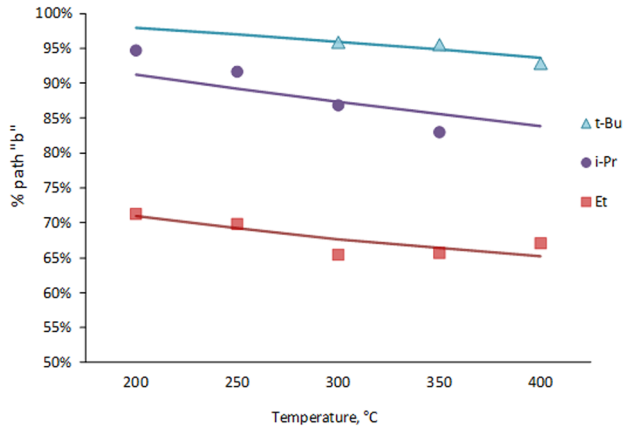

Figure 3. Preference for Path "*b*" depending on temperature for different acids with KOH treated ZrO_2 catalyst. Dots represent measured data. Solid lines represent the linear trendlines serving as the basis for the calculation of the activation energy difference between two pathways.

From these data, the activation energy difference, E^a_{diff}, between Path "*a*" and Path "*b*" was estimated based on the difference in the apparent reaction rates for the formation of mixed ketones with and without the labeled carbonyl group. Fitting the experimental data into the Arrhenius equation, $E^a_{diff} = -RT \ln(k_{Path\ a}/k_{Path\ b})$ yielded the E^a_{diff} values of 0.8 ± 0.1, 2.2 ± 0.5, and 3.6 ± 0.2 kcal/mol for the cross ketonization of acetic acid with propionic, isobutyric, and pivalic acids, respectively. Therefore, Path "*b*" is consistently favored over Path "*a*" for the carbonyl component derived from any acid that is more branched compared to acetic acid.

The difference in effective activation energies measured by this method, to which we refer henceforth as Method 1, thus compares the activation energies of the rate-limiting steps in Paths "*a*" and "*b*". Because the ketonization mechanism involves several steps, each mechanistic path may have its own rate-limiting step, which may not necessarily be shared. A rate-limiting step could be, for example, the activation of an enolic component as a result of the surface carboxylate enolization. It could as well be one of the subsequent steps after the enolization, such as a carbon−carbon bond formation in the bimolecular condensation step or carbon−carbon bond cleavage for the loss of CO_2 molecule.

Thus a critically important action in mechanism discrimination would be the separation of the enolization (enolic component activation) step from the subsequent steps. Remarkably, this turned out to be possible without isolation of the activated enolic component by using the method of competing reactions, to be called Method 2.

3.4. Method of Competing Reactions for Post Enolization Steps. As shown in Scheme 2, the enolic intermediate derived from acetic acid, $\mathbf{A_e}$, could react with the carbonyl component derived either from another acetic acid, $\mathbf{A_c}$, or from isobutyric acid, $\mathbf{B_c}$, to form either acetone, *m*/*z* 59, or methyl isopropyl ketone, *m*/*z* 86, respectively. The method of competing reactions[36] was applied to calculate the ratio of reaction rates, k_1/k_2, based on the ratio of products with *m*/*z* 59 to *m*/*z* 86. Because the experimental conditions were selected so as to provide only a partial conversion of acids, that is less than 10%, a large excess of unreacted acids present in the mixture was assured. It was further assumed that (1) the preliminary activation of the enolic component took place as a separate step; (2) the activated species $\mathbf{A_e}$ were formed at low concentrations, and (3) the activated species $\mathbf{A_e}$ then competitively reacted with acids **A** and **B** being present in excess. In this case the reaction kinetics can be described by a pseudofirst order on the enolic component while the acid concentration would remain constant. The ratio of reaction constants leading to products $\mathbf{A_eA_c}$ and $\mathbf{A_eB_c}$ was calculated as[36]

$$\frac{k_1}{k_2} = \frac{\ln[A_0] - \ln([A_0] - [A_eA_c])}{\ln[B_0] - \ln([B_0] - [A_eB_c])} \quad (1a)$$

where $\mathbf{A_0}$ and $\mathbf{B_0}$ are the initial acid concentrations and $\mathbf{A_eA_c}$ and $\mathbf{A_eB_c}$ are the measured product concentrations, that is products with *m*/*z* 59 and *m*/*z* 86. The derivation of eq 1a is provided in the Supporting Information.

From the temperature dependence of the above ratio at 200−300 °C, the difference in Arrhenius activation energies was calculated as

$$E^a_2 - E^a_1 = RT \ln(k_1/k_2) \quad (2a)$$

Experiments were conducted at three different molar **A**/**B** ratios of acids, 1:4, 4:1, and 9:1, resulting in the calculated activation energy differences of 2.6 ± 0.3, 2.8 ± 1.3, and 3.2 ± 0.6 kcal/mol, respectively. These values were not statistically different from each other, thus confirming the validity of the numerical value obtained. The average energy difference was thus calculated to be $E^a_2 - E^a_1 = E^a_{AeBc} - E^a_{AeAc} = 2.9 \pm 0.7$ kcal/mol.

Calculated by the same method, the average energy difference for the enolic component derived from isobutyric acid, $E^a_4 - E^a_3 = E^a_{BeBc} - E^a_{BeAc}$, was found to be 12.0 ± 0.5 kcal/mol. Modified eqs 1b and 2b were used to calculate the relative reaction rates, k_3 and k_4, of acetic and isobutyric acid carbonyl components with the same, isobutyrate-derived, enolic component and their respective activation energies (Scheme 2).

$$\frac{k_3}{k_4} = \frac{\ln[A_0] - \ln([A_0] - [B_eA_c])}{\ln[B_0] - \ln([B_0] - [B_eB_c])} \quad (1b)$$

where $\mathbf{B_eA_c}$ and $\mathbf{B_eB_c}$ are the measured product concentrations, that is products with *m*/*z* 87 and *m*/*z* 114.

$$E^a_4 - E^a_3 = RT \ln(k_3/k_4) \quad (2b)$$

The apparent activation energies for the formation of both symmetrical ketones were obtained earlier as discussed in

dx.doi.org/10.1021/cs3002989 | ACS Catal. 2012, 2, 1555−1562

Section 3.2. Because the formation of each of the symmetrical ketones shares the same enolic intermediate with the formation of a corresponding mixed ketone in either Path "*a*" or "*b*", it might be possible to obtain the complete set of activation energies for all four combinatorial products as shown in Table 1. A tempting solution would be to either add or subtract the

Table 1. Activation Energies for the Formation of All Ketones in a Cross-Ketonization of Isobutyric and Acetic Acids[a]

(Path "*a*")	B_eA_c 18.9 ± 0.7	B_eB_c 30.9 ± 0.5	
	A_eA_c 14.0 ± 0.3	A_eB_c 16.9 ± 0.6	(Path "*b*")

[a]kcal/mol.

energy difference obtained by eq (2) to or from the apparent activation energy of symmetrical ketones formation, which would give $E^a_2 = E^a_{AeBc} = 14.0 + 2.9 = 16.9$ kcal/mol, and $E^a_3 = E^a_{BeAc} = 30.9 - 12.0 = 18.9$ kcal/mol. However, this approach is valid only for a specific case when enolization is not the rate-limiting step. Otherwise, the activation energies estimated by these two methods may be reflecting the rate-limiting steps of different sections of the mechanistic pathway. It should be noted that Method 1 applies to the entire sequence of all steps of the ketonization mechanism including the enolization step, whereas Method 2 deals specifically with the post enolization steps only. Thus, additional steps were taken to ensure the correct matching of the results of these two methods.

The problem originates from the uncertainty of whether the enolic component activation has a higher energy barrier than the subsequent steps and so is picked up by Method 1. Two representative cases are illustrated in Figures 4a and 4b. When

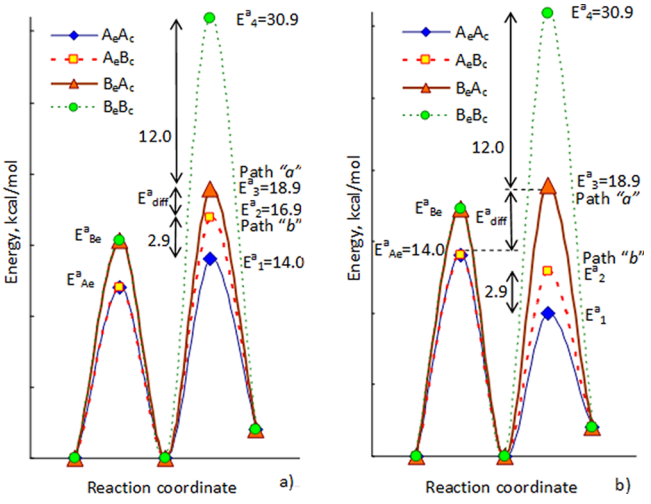

Figure 4. Energy profile for ketonization mechanism showing the enolization and the subsequent step when (a) the enolization is not the rate-limiting step, or (b) enolization is the rate-limiting step for Path "*b*" cross ketonization product, $\mathbf{A_eB_c}$, but not for the Path "*a*" product, $\mathbf{B_eA_c}$.

the enolization step is kinetically insignificant, that is, proceeds with a low activation energy (Figure 4a), the difference between Path "*a*" and "*b*" activation energies, E^a_{diff}, is equal to the difference between Reactions 2 and 3 (Scheme 2). In contrast, Figure 4b illustrates one of several alternative scenarios as an example, where the measured difference between Path "*a*" and "*b*" activation energies is due to the difference between the enolization energy for Path "*b*" and the activation energy for one of the subsequent steps of Path "*a*". In such a case, the measured E^a_{diff} does not have the same value as the difference between the activation energies of Reactions 2 and 3. Moreover, the exact values of E^a_1 and E^a_2 could not be determined in the example described by Figure 4b. However, Figure 4b must be dismissed on the consideration that $E^a_{diff.}$ in this case would be as high as 18.9 − 14.0 = 4.9 kcal/mol, which is significantly larger than the 2.2 kcal/mol obtained by Method 1. Combinatorial search for all other possible energy profile arrangements in the ketonization mechanism yielded the energy diagram depicted in Figure 4a as the only solution consistent with both methods.

After assuring the validity of Figure 4a, the absolute values for cross product activation energies under such conditions, that is, for only post enolization steps, were calculated as $E^a_{AeBc} = E^a_{AeAc} + 2.9 = 16.9$ kcal/mol and $E^a_{BeAc} = E^a_{BeBc} - 12.0 = 18.9$ kcal/mol (Table 1). For the reaction of isobutyric acid with acetic acid, the obtained value of $E^a_{diff} = 2.2 \pm 0.5$ kcal/mol by Method 1 matches the value of $E^a_3 - E^a_2 = 2.0 \pm 0.9$ kcal/mol obtained by the method of competing reactions. This difference between Path "*a*" and Path "*b*" was consistently observed and statistically significant. Thus, the successful cross-matching of two methods corroborated the hypothesis that the rate-determining step is not the activation of the enolic component, but one of the subsequent steps after its activation.

3.5. Critical Factors Governing Paths "*a*" and "*b*".

Factors resulting in the difference between Paths "*a*" and "*b*" reaction rates may include steric factors in the transition states of rate-limiting steps as well as the difference in the concentration of activated enolic components, $\mathbf{A_e}$ and $\mathbf{B_e}$. Reactions occurring prior to the rate-limiting step may still influence the reaction rate. As determined in Section 3.1, concentration of surface acetates and isobutyrates is approximately equal, but their ability for enolization may be different. The activation energy difference between the isobutyrate and the acetate enolization on the (111) surface of monoclinic zirconia estimated by density functional theory computations is 3.3 kcal/mol.[29] This value is close to the experimentally observed difference in the activation energies between Paths "*a*" and "*b*", but the enolization can now be excluded from the list of possible rate-limiting steps in view of the obtained kinetic results. However, the enolization might still influence the selectivity, for example, to mixed ketones vs symmetrical ketones.

At the same time, analysis of the data presented in Table 1 suggests significant steric factors in the ketonization mechanism. Thus reaction of the same enolic component with two different carbonyl components is sensitive to branching at the α carbon, resulting in a 2.9 kcal/mol activation energy difference for the same $\mathbf{A_e}$ enolic component with acetic and isobutyric carbonyl components, $\mathbf{A_c}$ and $\mathbf{B_c}$. The enolic component derived from isobutyrate, $\mathbf{B_e}$, is even more sensitive to the steric hindrance, resulting in a 12.0 kcal/mol activation energy difference with acetic and isobutyric carbonyl components. Reaction of the same carbonyl component with two different enolic components is also sensitive to steric factors. The observed difference in activation energies is 4.9 kcal/mol for $\mathbf{A_c}$ and 14.0 kcal/mol for $\mathbf{B_c}$ reactions with two competing enolic components (Table 1).

This mechanistically significant interaction of enolic and carbonyl components is consistent with the rate-limiting step occurring after enolization. The two obvious "candidates" for

dx.doi.org/10.1021/cs3002989 | *ACS Catal.* 2012, 2, 1555−1562

being rate limiting are condensation and decarboxylation. However, the method used in this study does not allow for distinguishing between these two options.

Because of experimental evidence that rules out enolization as the rate-limiting step in the ketonization mechanism, the factor determining the difference in reactivity of acetic vs isobutyric acids is not the acid's ability to enolize. The difference in reactivity may be explained now by the steric factor caused by branching at the α carbon of the carboxylic acids. If, for example, the true ketonization mechanism proceeds through a beta-ketoacid formation and decarboxylative decomposition, the steric repulsion of substituents during their rotation in the course of sp^3-sp^2 hybridization change (Scheme 3) would be responsible for imposing a kinetic

Scheme 3. Pathways for Cross-Ketonization Mechanism through a Beta-Ketoacid Formation and Decarboxylative Decomposition Showing Steric Repulsion of Substituents

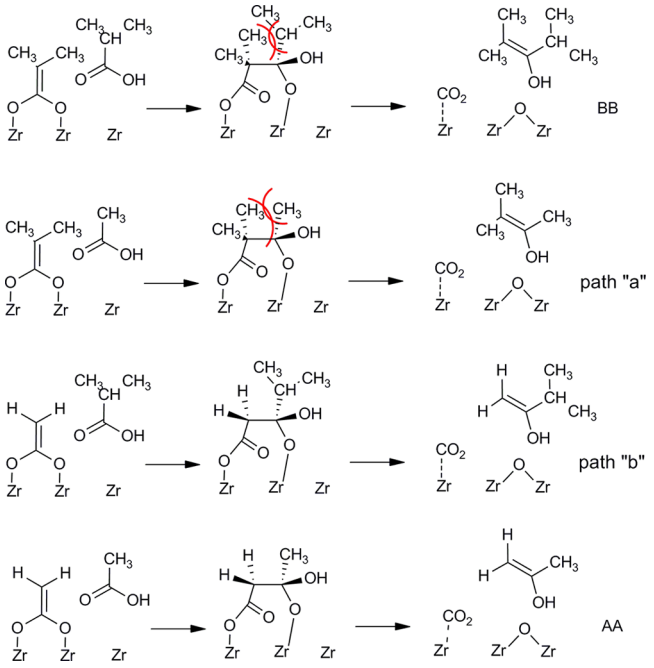

limitation. An increased repulsion occurs when isobutyrate serves as the enolic component for the formation of symmetrical ketone, **BB**, and the mixed ketone, $\mathbf{B_eA_c}$, by Path "*a*". However, without a specific experimental support, the assumption that decarboxylation is the rate-limiting step remains only as speculation.

4. CONCLUSIONS

Placing a pulsed microreactor inside a GC−MS instrument was shown to be a useful technique for measuring the reaction rates of catalytic carboxylic acid ketonization with a low amount of isotopically labeled compounds and a small amount of catalyst. The source of the acyl and alkyl group of the mixed ketone in the cross reaction between two different acids was traced depending on the carboxylic acid branching at the α carbon next to the carboxylic group. On the basis of the analogy with the classic aldol condensation, a concept of enolic and carbonyl components can be successfully applied to the ketonization mechanism. Carboxylic acid ketonization was found to be sensitive to steric factors caused by both the enolic and the carbonyl components. The more branched carboxylic acid tends to react as the carbonyl component serving as the source of the acyl group in the mixed ketone product according to Path "*b*". The difference between mechanistic Paths "*a*" and "*b*" for the formation of the cross-ketonization product was quantitatively measured and found to be 0.8 ± 0.1, 2.2 ± 0.5, and 3.6 ± 0.2 kcal/mol for the cross ketonization of acetic acid with propionic, isobutyric, and pivalic acids respectively.

The method of competing reactions was used to study reaction of the same enolic component with two different carbonyl components. For example, the enolic component derived from acetic acid, requires activation energy 2.9 ± 0.7 kcal/mol higher in the reaction with isobutyric acid vs reaction with acetic acid as the carbonyl component. The rate-limiting step appears to occur after the activation of the enolic component. It is assumed that the rate-limiting step is more likely associated with the loss of CO_2.

■ ASSOCIATED CONTENT

Supporting Information

Derivation of kinetic equations, tabulated data for Figures 1−3 and Method 2. This material is available free of charge via the Internet at http://pubs.acs.org.

■ AUTHOR INFORMATION

Corresponding Author

*Phone: (701) 777-5052. Fax: (701) 777-5181. E-mail: alexey.ignatchenko@gmail.com.

Funding

Measurements were carried out with the GC−MS instrument acquired thanks to the U.S. Army Contract No. W911NF-07-C-0046. E.I.K. thanks UND Chemistry Department for continuous support.

Notes

The authors declare no competing financial interest.

■ ACKNOWLEDGMENTS

Use of the EERC Fuels lab and other EERC research facilities is greatly acknowledged.

■ REFERENCES

(1) Schommer, C.; Ebel, K.; Dockner, T.; Irgang, M.; Hoelderich, W.; Rust, H. U.S. Patent 4950763, 1990.
(2) Cryberg, R. L.; Bimber, R. M. U.S. Patent 4570021, 1986.
(3) Renz, M. *Eur. J. Org. Chem.* **2005**, 979−988.
(4) Mekhemer, G. A. H.; Halawy, S. A.; Mohamed, M. A.; Zaki, M. I. *J. Catal.* **2005**, *230*, 109−122.
(5) Hwang, Y-L; Bedard, T. C. Ketones. In *Kirk-Othmer Encyclopedia of Chemical Technology*, 5th ed.; John Wiley & Sons: New York, 2005; Vol. *14*, pp 1−47.
(6) Nicholson, J. W.; Wilson, A. D. *J. Chem. Ed.* **2004**, *81*, 1362−1366.
(7) Friedel, C. *Justus Liebigs Ann. Chem.* **1858**, *108*, 122−125.
(8) Fittig, R. *Justus Liebigs Ann. Chem.* **1859**, *110*, 17−23.
(9) Imanaka, T.; Tanemoto, T.; Teranishi, S. *Proceedings of the 5th International Congress on Catalysis*, Palm Beach, FL, 1972; Hightower, J.W., Ed.; Elsevier: Amsterdam, The Netherlands, 1973; Vol. *1*, p 163.
(10) Pestman, R.; Koster, R. M.; Dujine, A.; Pieterse, J. A. Z.; Ponec, V. *J. Catal.* **1997**, *168*, 265−272.
(11) Jewur, S. S.; Kuriacose, J. C. *Indian Chem. Manuf.* **1974**, *12*, 13−15.
(12) Nagashima, O.; Sato, S.; Takahashi, R.; Sodesawa, T. *J. Mol. Catal. A* **2005**, *227*, 231−239.
(13) Bongard, W.; Wilms, H. German Patent DE 956498, 1956.

(14) Parbuzina, I. L.; Sosnina, I. E.; Ivanova, T. N.; Balandin, A. A. *Doklady Akademii Nauk SSSR* **1967**, *173*, 606−608.
(15) Rubinshtein, A. M.; Yakerson, V. I.; Lafer, L. I. *Kinet. Katal.* **1964**, *5*, 319−323.
(16) Okumura, K.; Iwasawa, Y. *J. Catal.* **1996**, *164*, 440−448.
(17) Leicester, J.; Redman, M. J. *J. Appl. Chem.* **1962**, *12*, 357−366.
(18) Galwey, A. K. *J. Chem. Soc.* **1965**, 6188−6194.
(19) Gaertner, C. A.; Serrano-Ruiz, J. C.; Braden, D. J.; Dumesic, J. A. *J. Catal.* **2009**, *266*, 71−78.
(20) Rajadurai, S. *Catal. Rev. - Sci. Eng.* **1994**, *36*, 385−403.
(21) Jewur, S. S.; Swaminathan, R.; Kuriacose, J. C. *Indian J. Chem., Sect. A* **1976**, *14A*, 279−280.
(22) Rajadurai, S.; Kuriacose, J. C. *Mater. Chem. Phys.* **1987**, *16*, 17−29.
(23) Plint, N. D.; Coville, N. J.; Lack, D.; Nattrass, G. L.; Vallay, T. *J. Mol. Catal. A* **2001**, *165*, 275−281.
(24) Hendren, T. S.; Dooley, K. M. *Catal. Today* **2003**, *85*, 333−351.
(25) Parida, K.; Mishra, H. K. *J. Mol. Catal. A* **1999**, *139*, 73−80.
(26) Ignatchenko, A. V.; King, M. M.; Liu, Z.; Whiddon, C. W. U.S. Patent 7452841, 2008.
(27) Jayamani, M.; Pillai, C. N. *J. Catal.* **1984**, *87*, 93−97.
(28) Gonzalez, F.; Munuera, G.; Prieto, J. A. *J. Chem. Soc. Faraday Trans. 1* **1978**, *74*, 1517−1529.
(29) Ignatchenko, A. V. *J. Phys. Chem. C* **2011**, *115*, 16012−16018.
(30) Kuriacose, J. C.; Jewur, S. S. *J. Catal.* **1977**, *56*, 330−341.
(31) Noszko, L.; Szammer, J.; Szabolcs, A.; Otvos, L. *Radiochem. Radioanal. Lett.* **1970**, *5*, 265.
(32) Mertig, C. P. *Arch. Biquim., Quim. Farm.* **1968**, *14*, 103−130.
(33) Lee, C. C.; Spinks, J. W. T. *J. Org. Chem.* **1953**, *18*, 1079−1086.
(34) Ignatchenko, A.; Hill, J.; Gray, J.; Nealon, D.; Dushane, R. *Proceedings of 18th North American Catalysis Society Meeting*, Cancun, Mexico, 2003; p 169.
(35) Ignatchenko, A.; Nealon, D.; Dushane, R.; Humphries, K. *J. Mol. Catal. A* **2006**, *256*, 57−74.
(36) Bast, K.; Christl, M.; Huisgen, R.; Mack, W. *Chem. Ber.* **1973**, *106*, 3312−3344.